Reservoir characterization using Seismic sparse-layer reflectivity inversion methods: A case study

Ajay Pratap Singh[1,], S.P. Maurya[1], M.K. Srivastava[1] and Ravi Kant[1]*
[1]*Department of Geophysics, Banaras Hindu University, Varanasi, India-221005*
*ajaygeop21@bhu.ac.in

Keywords

Seismic inversion, reservoir characterization, acoustic impedance.

Abstract

For the purpose of developing, managing, and optimizing a reservoir's output, accurate reservoir characterization is a crucial step. Reservoir characterization must be dynamic in order to attain accuracy and guarantee that all information available at any given time is incorporated into the reservoir model. But in order to do so, one must first create a static model. Static model is a straightforward representation of the reservoir at a specific time in order to begin. With the availability of newly acquired petrophysical, seismic, and production data, the reservoir model is adjusted to account the changes in the reservoir. The improved model would serve as a more accurate gauge of the state of reservoir at the moment. In the present study, a reservoir characterization using sparse layer reflectivity (SLR) inversion has been introduced. The inversion is carried out by defining a set of functions to characterize reflectivity patterns and constructing the seismic trace as a superposition of these patterns. A small number of reflection responses are discovered through basis pursuit decomposition, and these responses are combined to produce the seismic trace. The method is first tested for the composite trace extracted near to well location. The qualitative and quantitative analysis of composite trace shows that the correlation between inverted and original impedance is 0.99 with 0.041 RMS error. Thereafter, the post-stack seismic data from the Blackfoot field, is inverted into acoustic impedance (AI) and interpretation has been done. The inverted section shows that AI varies between 6000-18000m/s*g/cc with very high-resolution subsurface information. A low impedance anomaly has been noticed near to 1050-1065ms time interval and interpreted as a sand channel. The SLR inversion approach is particularly effective at identifying thin layers that other seismic inversion techniques can't retrieve.

Introduction

Seismic reservoir characterization uses seismic and well log data to infer the underlying rock and fluid parameters, such as velocities, density, porosity, mineral fractions, and fluid saturations. This task is a mathematical inverse problem that uses optimization techniques to try to reduce the discrepancy between the anticipated seismic response and the measured data in order to identify the most probable reservoir models (Zhang and Castangna, 2011). Pre- and post-processing of the seismic data as well as parameter calibrations are typically necessary for the traditional model-driven procedures based on physical relations.

Yuan and Wang (2013) made use of a sparse seismic inversion method that is renowned for its ability to produce reflectivity solutions with a wider bandwidth, even outside the original seismic signal's frequency range. The principle of sparsity, which refers to the notion that seismic reflectivity models may be described using just a minimal number of significant coefficients or basis functions, is used in these techniques. However, incorporating existing knowledge into the seismic trace reflectivity inversion may be challenging. One popular approach for incorporating prior knowledge involves building an initial model that is biased by the information available at the moment and allowing the inversion process to enhance it until it converges to a solution. It is usual practice to acquire an initial estimate for reflectivity inversion by spatially interpolating well logs along with specified horizons. When building a beginning model for reflectivity inversion, a problem emerges when these horizons must be identified on the original seismic data. Horizon picking is the act of manually selecting and tracking seismic reflections that correspond to specified geological or stratigraphic structures.

Matching pursuit decomposition (MPD) and Basis pursuit decomposition (BPD) can be integrated into the reservoir characterization process using sparse layer reflectivity inversion methods to improve the accuracy and effectiveness of the analysis. MPD helps in identifying the key waveforms associated with specific subsurface features, while BPD enables the estimation of the reflectivity series for each subsurface layer. By combining the results of MPD and BPD, it becomes possible to construct a sparse representation of the

seismic data that accurately represents the subsurface reflectivity variations. This sparse representation can then be further utilized in sparse layer reflectivity methods to estimate important reservoir parameters, such as layer thickness, velocity, and impedance contrast.

Matching Pursuit Decomposition (MPD) is a signal processing approach that may be used to deconstruct a seismic trace into a superposition of reflectivity patterns detected in existing well control and generated from it (Sui and Ma, 2020). MPD is a type of sparse decomposition in which a signal is represented using a minimal number of basis functions. Pereg et al. (2017) used Matching pursuit decomposition with following steps (1) compares a wavelet dictionary to a seismogram to determine the location, scale (i.e., centre frequency), and amplitude of the best-fit wavelet, (2) subtracts the best-fit wavelet and records its characteristics in a table, and (3) repeats the processes on the residual trace until the residual energy falls below a predetermined threshold.

MPD heavily relies on the choice of the dictionary or the set of components used for signal representation. The quality and appropriateness of the dictionary can significantly impact the accuracy of the representation. In cases where an appropriate dictionary is not available or difficult to construct, the performance of MPD can be suboptimal. Due to its capacity to handle interferences between dictionary components, computational effectiveness, and strong lateral stability even with non-orthogonal dictionaries, Basis pursuit decomposition (BPD) has an edge over MPD (Duval and Peyré, 2017). In situations where signal components overlap or the dictionary is not absolutely orthogonal, these characteristics make BPD a potent tool for sparse signal decomposition and representation. In this paper, we explore the use of BPD to perform seismic inversion (Chen et al., 2001) decomposes the seismic trace using a nonorthogonal wavelet dictionary made up of even and odd thin layer seismic responses. We investigate the usage of a seismic wavelet and a wedge-model of reflection coefficient pairs as a very basic dictionary of reflection patterns. Using Basis pursuit decomposition (BPD) with a wedge dictionary results in a sparse layer inversion. In this study, we will compare BP sparse-layer inversion (BPI) to conventional sparse-spike inversion using synthetic and real data to assess BPI's capacity to resolve thin beds and disclose tiny stratigraphic features.

Methodology

The forward model is considered to be a simple convolution of a stationary seismic wavelet and the reflectivity for simplicity. Thus, the seismic trace $s(t)$ is given by

$$s(t) = w(t) * r(t) + n(t) \qquad (1)$$

where w(t) represents the seismic wavelet, $r(t)$ represents the reflectivity series, and $n(t)$ represents noise. The earth structure is assumed to be properly described by a sequence of planar horizontal layers of constant impedance with reflections created at the borders between consecutive levels (Helgesen et al., 2000). To make the inversion even easier, we assume that the wavelet is known.

It is believed that the subsurface is made up of horizontal isotropic homogenous layers. Each post-stack seismic image trace is thought to represent the convolution of a seismic wavelet with a reflectivity series. The convolutional model (equation 1) may also be developed for seismic reflection data to allow the seismic wavelet to fluctuate temporally.

$$S = Wr + n \qquad (2)$$

where S is a column vector that represents the seismogram, r is a column vector that represents the reflectivity series, W is a diagonal wavelet kernel matrix, and n is a column vector that represents noise. The well-known version of this convolutional procedure is as follows:

$$d = Gm + n \qquad (3)$$

where d denotes the data vector, m the model parameters, G the kernel, and n the noise.

In order to get the parameters in equation (3), basis pursuit (BP) must simultaneously minimise the L_2 norm of the error term and L_1 norm of the solution.

$$Min[||d - Gm||_2 + \lambda||m||_1] \qquad (4)$$

Two impulse functions, $c\square(t)$ and $d\square(t + \Delta t)$, where $n\Delta(t)$ is the time thickness of the thin-bed, Δt is the sampling rate, and c and d are the two reflection coefficients, can be used to represent the top and bottom reflectors of a layer (Russell and Hampson, 1991). Each reflector pair is split into one even pair (r_e) and one odd pair (r_o), with associated coefficients a and b, that range from -1 to +1 times a scale factor. These coefficients may be written as equations 5 and 6:

$$\begin{aligned} r_e &= \square(t) + \square(t + n\Delta t); \\ r_o &= \square(t) - \square(t + n\Delta t); \end{aligned} \qquad (5)$$

$$c\square(t) + d\square(t + n\Delta t) = ar_e + br_o \qquad (6)$$

Shifting the reflectivity pair down the time axis with $m\Delta t$, where m varies from one to the number of samples in the seismic trace, creates the reflector kernel matrix

for the reflectivity pair. As a result, the formula for each even wedge reflectivity is:

$$r_e\,(t,m,n,\Delta t) = \square(t - m\Delta t) + \square(t - m\Delta t + n\Delta t). \quad (7)$$

With the exception of polarised dipoles, the odd wedge reflectivity follows the same pattern as the even wedge, written as

$$r_o\,(t,m,n,\Delta t) = \square(t - m\Delta t) - \square(t - m\Delta t + n\Delta t). \quad (8)$$

Any reflectivity series may be thought of as the sum of even and odd wedge reflectivity patterns as illustrated in equation 9.

$$r(t) = \sum_{n=1}^{N}\sum_{m=1}^{M}\left(a_{n,m} * r_e\,(t,m,n,\Delta t) + b_{n,m} * r_o\,(t,m,n,\Delta t)\right) \quad (9)$$

The seismic trace is represented by the left side of equation 9 when it is convolved with the wavelet, w, and the sum of the even and odd wedge seismic responses is represented by the right side of equation 9, as illustrated in equation 10:

$$s(t) = \sum_{n=1}^{N}\sum_{m=1}^{M}\left(a_{n,m} * wr_e\,(t,m,n,\Delta t) + b_{n,m} * wr_o\,(t,m,n,\Delta t)\right) \quad (10)$$

where the seismic responses of the wedge reflectivity pairs are w_{re} and w_{ro}. Any seismic trace may be seen as a collection of wedge seismic dictionary pieces. The decomposition of reflectivity into wedge reflector pairs and that of the seismic trace into wedge seismic responses share precisely the same scalar coefficients $a_{n,m}$ and $b_{n,m}$, assuming that the seismic trace is appropriately scaled to reflection coefficient magnitudes.

By resolving equation 10, BPI may be used to determine the coefficients $a_{n,m}$ and $b_{n,m}$. The inverted series may be derived by adding the wedge reflectivity models with coefficients $a_{n,m}$ and $b_{n,m}$, as shown in equation 9, since equations 9 and 10 have the same coefficients. If the waveform amplitudes are appropriately scaled to reflection coefficients, the coefficients $a_{n,m}$ and $b_{n,m}$ are of the same magnitude as the reflection coefficients since the reflection coefficients and dipole reflector pairs are defined with values ranging from -1 to 1.

Result

Post-stack seismic inversion uses NMO-corrected and layered CMP seismic data. The initial stage in this inversion process is wavelet extraction. Wavelet extraction is followed by well-log to seismic correlation, which is done for each well separately.

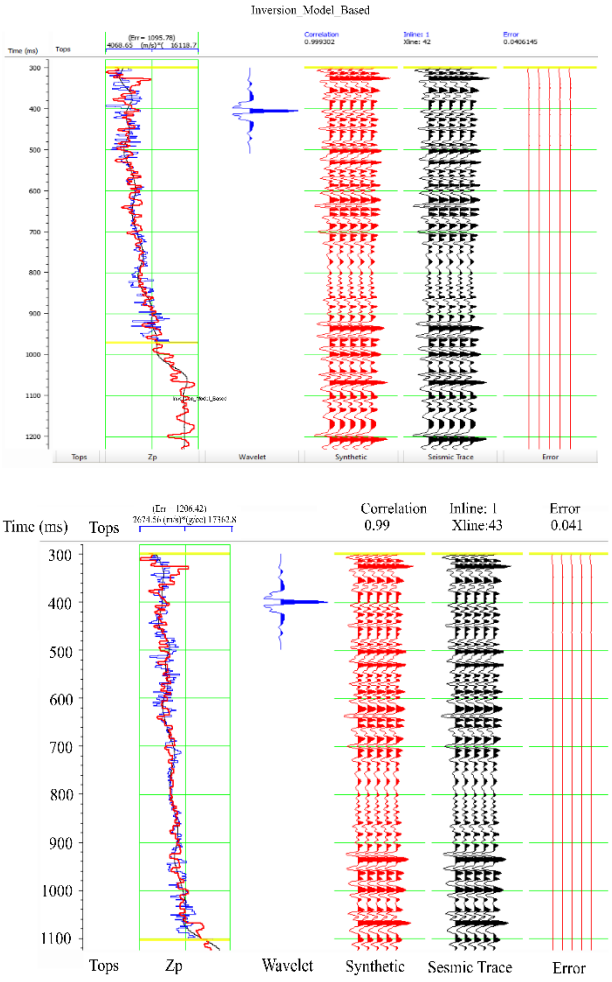

Figure 1: (a) Inversion analysis based on the Model-based approach reveals a high correlation of 0.99 and an error margin of 0.040, indicating strong alignment. (b) SLR analysis showcases a robust correlation of 0.99 and an error of 0.041, further emphasizing the accuracy.

The correlation process is used as follows:

1. The seismic trace closest to the well site is compared to a synthetic trace created using well log data;
2. The data is time-stretched and time-constrained to align the seismic and well-log reflectors;
3. Between the seismic and modified well-log synthetic traces, correlation coefficient and RMS Error are calculated.

The presence of a loosely compacted formation in the region becomes evident through the observation of relatively low impedance values. This characteristic

points towards the subsurface area with less dense material, possibly indicating a distinct geological feature. The evaluation of the Inversion analysis, encompassing both the model-based and SLR methods, reveals a remarkable correlation coefficient of 0.99. This signifies a robust alignment between the derived results and the original data. Notably, the associated error values stand at 0.040 for the model-based approach and 0.041 for the SLR method. Of particular interest is the nuanced distinction between these two techniques. The SLR method emerges as slightly superior, displaying a marginally smaller error margin compared to the model-based approach. This subtle difference reinforces the SLR's capability to provide a more refined interpretation, enhancing our insights into the underlying geological complexities.

Crossplot between P-impedance (original log) and P-impedance (inverted log) is displayed in Figure 2. In the crossplot, r square represents the fraction of the variation in the dependent variable that can be predicted by the independent variable. The crossplot's scatter point lie very close to best fit line which shows that the SLR inversion method has been performed well.

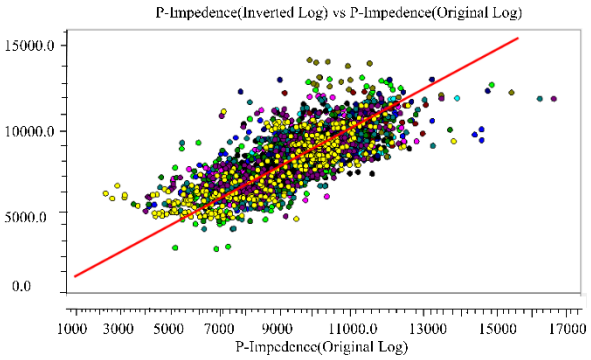

Figure: 2 Crossplot of P-impedance (original log) and P-impedance (inverted log).

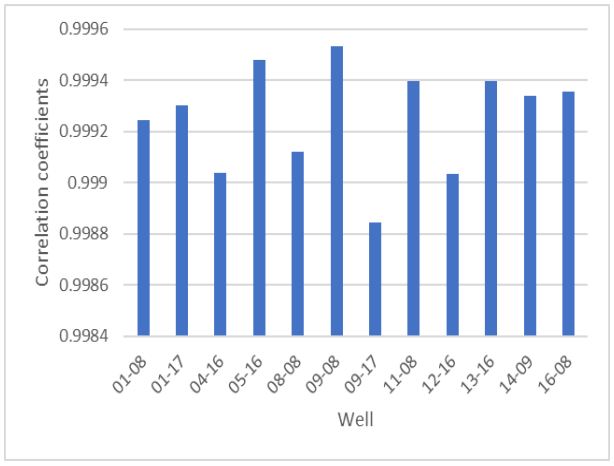

(a)

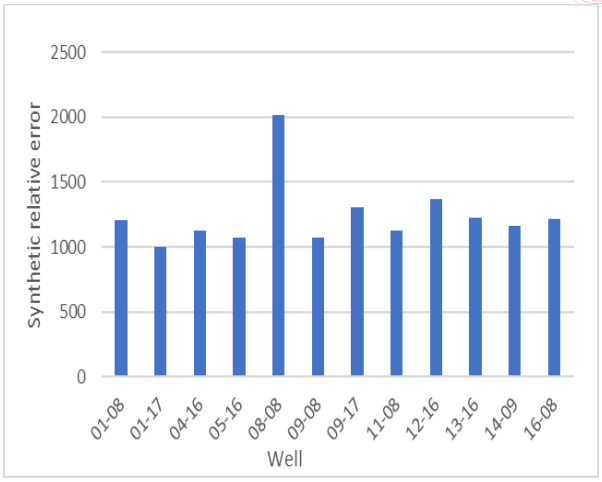

(b)

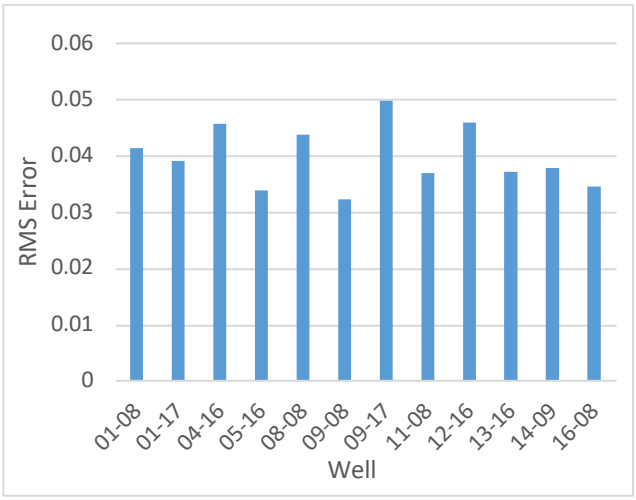

(c)

Figure: 3 Variation in (a) correlation coefficient, (b) synthetic relative error and (c) root mean square error for all available wells.

A correlation of inverted and real impedance is constructed to cross-validate the inversion results in (Figure 3). The variation in point distribution shows that the inverted impedances are extremely close to the real impedance for virtually all wells.

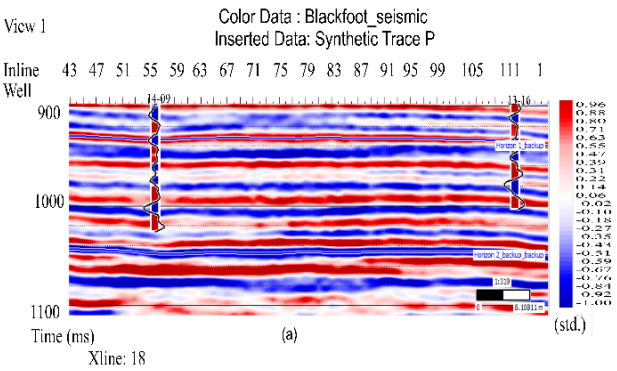

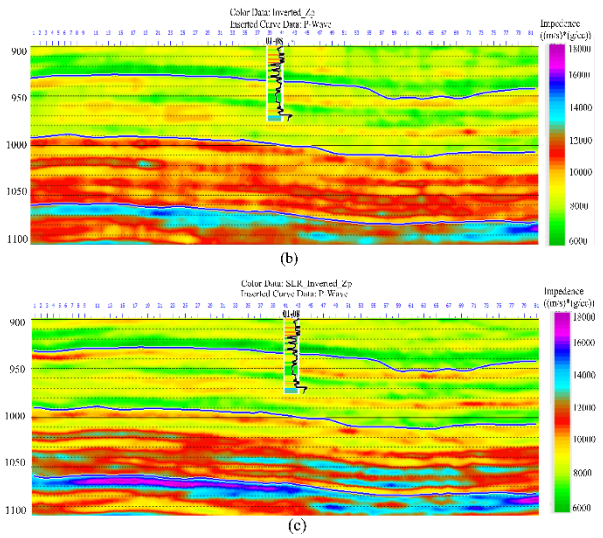

Figure 4: (a) Seismic data collected after the stack. (b) Inverted impedance section using model-based inversion method. (c) Inverted impedance section using SLR inversion method.

Figure 4(a) depicts the post-stack seismic section, while Figure 4(b) depicts the inverted section using SLR inversion method. The analysis of the impedance sections obtained from both the inverted model and the sparse layer reflectivity (SLR) technique has provided valuable insights into the subsurface properties. Notably, within the approximately 1060 ms time interval, a distinct region of reduced P-impedance becomes evident. This observation is particularly significant as it suggests the potential presence of a reservoir zone characterized by these lower impedance values. Intriguingly, while both methods shed light on this intriguing low-impedance zone, the SLR technique produce high-resolution subsurface imaging and detection of thin layers that are typically overlooked by other seismic inversion methods. The refined results yielded by SLR underscore its efficacy in capturing subtle variations and complexities within the seismic data. However, this is only a preliminary interpretation, and further information is required to characterize the reservoir.

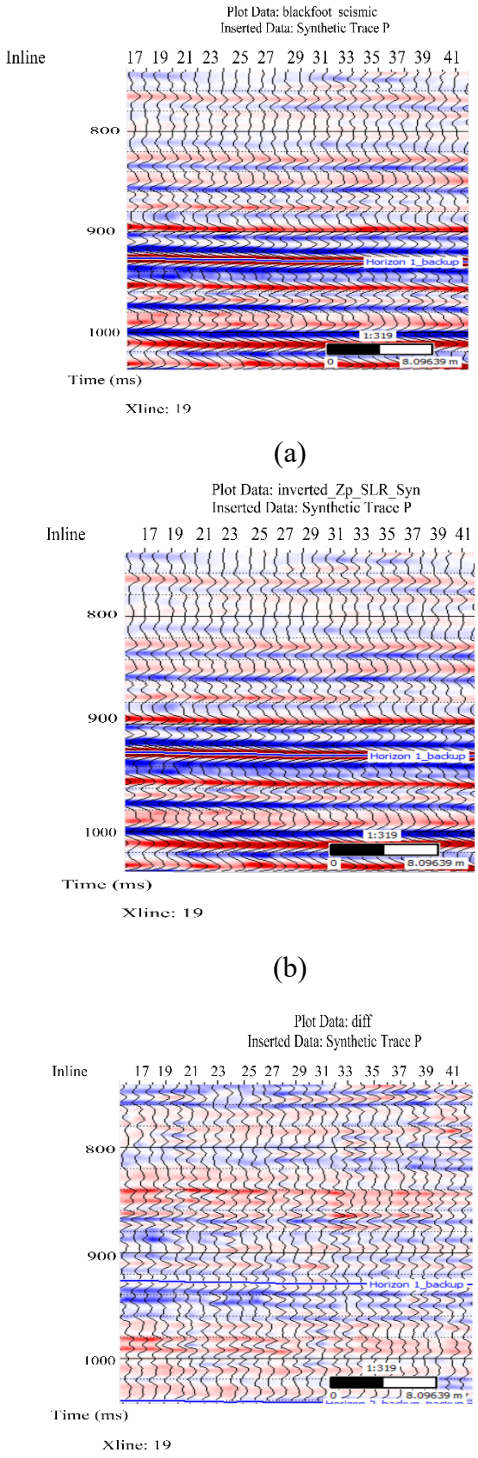

Figure 5: (a) Blackfoot seismic synthetic traces (b) Inverted acoustic impedance SLR synthetic traces (c) difference between Blackfoot synthetic and SLR synthetic

In Figure 5(a) shows the Blackfoot seismic section and 5(b) shows the inverted impedance section using SLR method. The difference between these two is shown in 5(c). It is evident from the difference that there is very less difference between the two inserted data which

clearly depicts the effectiveness of the SLR inversion method for post stack seismic data from Blackfoot.

Figure 6 depicts a impedance slice at 1065ms time interval. This slice depicts the horizontal fluctuation of the subsurface acoustic impedance. A further critical step is the creation of the slices, which indicate the horizontal variation in the acoustic impedance and, consequently, any horizontal change in the reservoir zone. Further observation reveals that the reservoir zone shifts from the SW to the NE.

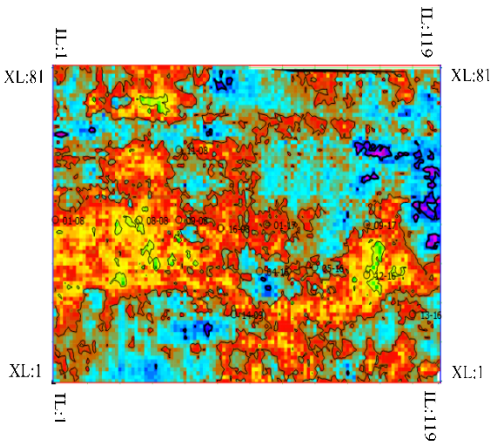

Figure 6: Impedance slice at 1065ms time interval.

Conclusion

In this paper, a variety of petrophysical parameters such as impedance and velocity are calculated through seismic sparse layer reflectivity inversion, which is relatively rapid and produces better results than other inversion methods. The analysis of sparse reflectivity inversion shows a very good correlation of 0.99 and a error of 0.041. Furthermore, the inversion of the full seismic section for impedance reveals a relatively low impedance that fluctuates between 6000 and 18000 m/s*g/cc in the region, indicating the presence of loose formation in the area. Thereafter, seismic synthetic traces and sparse layer reflectivity synthetic traces are performed. The difference between these two is very small, which clearly depicts the effectiveness of the sparse layer reflectivity inversion method. Furthermore, an impedance slice is generated, which shows the horizontal fluctuation of the subsurface acoustic impedance. SLR can yield high-resolution estimates of each subsurface layer's reflectivity series. Sparse layer reflectivity allows for a more complete and exact characterization of the reservoir by recording fine-scale variations in reflectivity, such as thin layers, small stratigraphic changes, or fault-related characteristics. This greater resolution aids in the identification of prospective hydrocarbon-bearing zones as well as the characterization of reservoir heterogeneities.

References

Zhang, R. and Castagna, J., 2011. Seismic sparse-layer reflectivity inversion using basis pursuit decomposition. *Geophysics*, *76*(6), pp. R147-R158.

Yuan, S. and Wang, S., 2013. Spectral sparse Bayesian learning reflectivity inversion. *Geophysical Prospecting*, *61*(4), pp.735-746.

Sui, Y. and Ma, J., 2020. Blind sparse-spike deconvolution with thin layers and structure. *Geophysics*, *85*(6), pp. V481-V496.

Helgesen, J., Magnus, I., Prosser, S., Saigal, G., Aamodt, G., Dolberg, D. and Busman, S., 2000. Comparison of constrained sparse spike and stochastic inversion for porosity prediction at Kristin Field. *The Leading Edge*, *19*(4), pp.400-407.

Russell, B. and Hampson, D., 1991. Comparison of poststack seismic inversion methods. In *SEG Technical Program Expanded Abstracts 1991* (pp. 876-878). Society of Exploration Geophysicists.

Chen, S. S., D. L. Donoho, and M. A. Saunders, 2001, Atomic decomposition by basis pursuit: Society for Industrial and Applied Mathematics Review, 43, no. 1, 129–159.

Duval, V. and Peyré, G., 2017. Sparse spikes super-resolution on thin grids II: the continuous basis pursuit. *Inverse Problems*, *33*(9), p.095008.

Pereg, D., Cohen, I. and Vassiliou, A.A., 2017. Multichannel sparse spike inversion. *Journal of Geophysics and Engineering*, *14*(5), pp.1290-1299.

Acknowledgments

S.P. Maurya, one of the authors, expresses gratitude for the support received from the financial organizations UGC-BSR (M-14-0585) and IoE BHU (Dev. Scheme no. 6031B). In addition, we acknowledge the academic licenses for Matlab (2022b) and Norsar (full package), respectively, from www.mathworks.com and www.norsar.no. This work couldn't be done without their help.